

# Nanomaterials for implantable batteries to power cardiac devices

T. Zhang<sup>a</sup>, Z. Li<sup>a</sup>, W. Hou<sup>b</sup>, Y. Yang<sup>a,\*</sup>

<sup>a</sup> Department of Applied Physics and Applied Mathematics, Columbia University, New York, NY, 10025, USA

<sup>b</sup> National United Engineering Laboratory for Biomedical Material Modification, Dezhou, Shandong, 251100, China



## ARTICLE INFO

### Article history:

Received 2 September 2019

Received in revised form

15 November 2019

Accepted 20 November 2019

Available online 28 November 2019

### Keywords:

Implantable batteries

Nanomaterials

Energy density

Energy storage

## ABSTRACT

Batteries have been used in various biomedical devices, such as neurostimulators, cardiac pacemakers, and implantable cardiac defibrillators. Compared to applications in electronics and electric vehicles, those implantable batteries need to be extremely safe and stable as they are placed inside human bodies to play a vital role in curing human diseases. They also need to have high energy density to save volume and weight in the limited space inside organs, such as heart ventricles. Not only that, complete packaging with no leakage possibility and extremely low self-discharge rate are also required to ensure the safe operation of devices without interruption for an 8–10 years battery life. These requirements are considerably demanding, and primary batteries are widely used in biomedical batteries to meet those requirements. Especially for cardiology applications, Li-CF<sub>x</sub> and Li-SVO (silver vanadium oxide) batteries have been used in industry for decades, and several improvements have been made to push overall battery performance to a theoretical limit. With recent progress made in enhanced treatment methods, such as communication functions among multiple leadless pacemakers for a more accurate sensing mechanism, those devices require even higher power input in order to drive new functions without losing life expectancy. In this review, we reviewed principles and recent progress on using nanomaterials in these battery systems for biomedical applications, such as how to further improve electrochemical performance and increase the reversibility of these battery systems as a potential solution to prolong their longevity inside human bodies.

© 2019 Published by Elsevier Ltd.

## 1. Introduction

Batteries are electrochemical devices that convert energy between the form of electricity and chemical bonds. They have been widely used for portable electronics, vehicle electrification, and grid-level energy storage. Besides these well-known markets, the biomedical application is a fast-growing field for batteries. In biomedical applications, batteries provide power for various apparatus from non-invasive sensors on skin surfaces to implantable devices inside the human body. These implantable devices distribute around multiple key organs, such as neurostimulators in the brain, cochlear implant, cardiac pacemaker, cardiac defibrillator, drug delivery system, and bone growth generator (Fig. 1) [1]. Compared to other applications, there are special requirements for implantable batteries. First, they need to be extremely safe as they are placed inside the human body. Secondly, they need to have high-energy density to save volume and weight in the limited space

in human body. Third, there cannot be any potential leakage considering the great risk of chemical contamination inside the human bodies. Last but not least, the self-discharge rate needs to be negligible so that the energy stored inside will not fade by itself.

These requirements are extremely demanding. For example, cardiac pacemakers and defibrillators not only require a stable and reliable operating power supply for an average 9 years with less than 0.25% annual self-discharging rate, but also need to provide pulse current up to 280 mA. To meet the target of such high energy density, primary batteries are widely used since they can provide theoretical energy density 50%–5X higher than secondary batteries, such as Li-ion batteries. Another reason why secondary batteries are not broadly used is their potential risk in heat generation and capacity lost along with charge/discharge cycles inside bodies. Hence primary batteries are more commonly used today despite their higher unit cost and limited longevity. Especially lithium-carbon monofluoride (Li/CF<sub>x</sub>), lithium-silver vanadium oxide (Li/SVO), lithium-iodine (Li/I<sub>2</sub>), and lithium manganese dioxide (Li/MnO<sub>2</sub>) are widely used for implantable batteries, as they have ultrahigh-energy densities (Table 1). For example, Li/CF<sub>x</sub> batteries

\* Corresponding author.

E-mail address: [yy2664@columbia.edu](mailto:yy2664@columbia.edu) (Y. Yang).

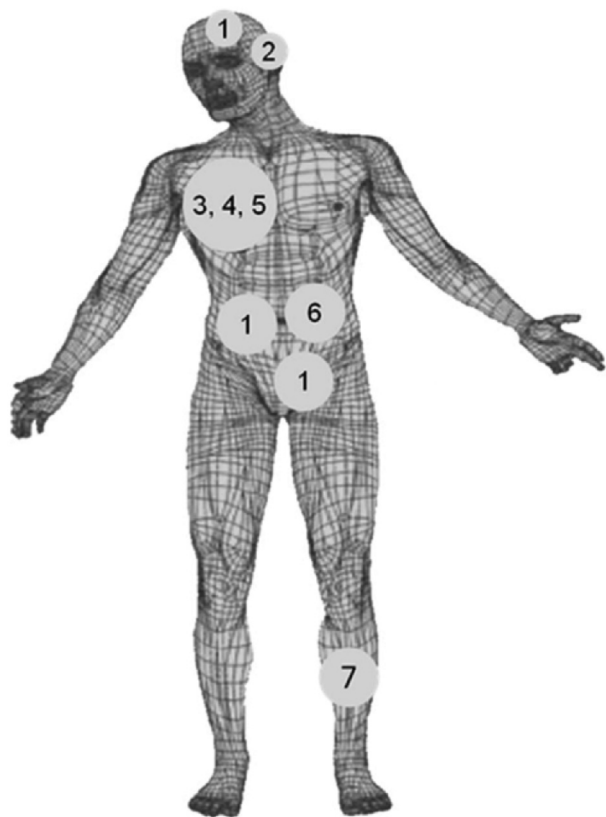


**Fig. 1.** Common implantable medical devices that use primary lithium batteries, as the main power source. (1) Neurostimulator. (2) Cochlear implant. (3) Pacemaker. (4) Implantable cardiac defibrillator. (5) Cardiac resynchronization device. (6) Drug delivery system. (7) Bone growth generator [1]. Adapted with permission from [1].

**Table 1**  
Primary batteries used in implantable medical devices.

Battery System	Nominal Cell Potential	Theoretical specific capacities of anode (mAh/g)	Theoretical specific capacities of cathode (mAh/g)	Theoretical energy densities (Wh/kg)	Practical energy densities (Wh/kg)
Li/I <sub>2</sub>	2.8	3861	211	560	210–270
Li/MnO <sub>2</sub>	3.0	3861	308	857	270 (low rate) 230 (high rate) [2]
Li/CF <sub>x</sub>	3.0	3861	864	2119	440[2]
Li/SVO	3.2	3861	315	932	270[2]
C/LiCoO <sub>2</sub>	3.9	372	180 <sup>a</sup>	752	200–250

<sup>a</sup> Based on high voltage LiCoO<sub>2</sub> charged to 4.4 V vs. Li<sup>+</sup>/Li.

have an open circuit voltage of 3.0 V and a theoretical energy density of 2119 Wh/kg, which is much higher than ~500 Wh/kg of Li-ion batteries.

Although high energy-density primary batteries have been applied to provide continuous power for medical devices, in order to help treat and cure several diseases, a constant invention of new treatment methods integrated with more complex sensing mechanism requires even more power from their power source and urge the development of higher capacity power systems. Several innovative cathode structures, separator/electrolyte modifications, and novel synthesis methods have been developed and tested to improve their electrochemical performance. For example, a hybrid CF<sub>x</sub> and SVO cathode was developed in recent years to take advantage of both the ideal energy density of CF<sub>x</sub> and the excellent power capability of SVO cathodes. Hence, small implantable medical devices can be powered for years without replacement [3]. A similar approach also applies to the CF<sub>x</sub>/MnO<sub>2</sub> hybrid cathode to

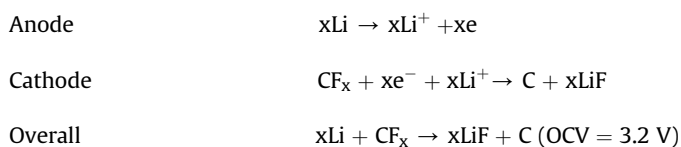
reduce the heat generation, eliminates voltage delay, and reduces cell cost [4].

Other approaches have also been examined on primary lithium batteries to further improve energy densities and extend their longevity, but in comparison to the fast-growing Li-ion battery industry, those high-density primary batteries have drawn significantly less attention. Besides, the recent breakthrough in micro-scale energy generator based on microelectromechanical systems, such as piezoelectric material, provides a potential solution to charge a micro battery inside human bodies, thus brings up the possibilities to implement a high-energy-density rechargeable battery, which technically could maximally prolong the device longevity and save patients' the trouble to replace the implanted medical device when its battery is drained. For applying current to high-power primary battery, such as Li/SVO to a micro rechargeable battery, the main challenge is the irreversibility of lithium intercalation, and it could hardly be improved through simply modifying the battery structure. Meanwhile, with the recent progress made toward nanotechnology and nanofabrication techniques, we're now given a new tool to improve the battery performance. Even though all battery types mentioned above in Table 1 have been applied in the industry and studied for possible enhancement in electrochemical performance, some types, such as Li/MnO<sub>2</sub> and C/LiCoO<sub>2</sub> have drawn comparably less attention for its physical limitation, actual cost, and manufacturing difficulty meeting higher power and energy density requirements for future biomedical devices. In this review, we focus on exploring the recent nanoscale material properties and seeking improvement in electrochemical performance for Li/CF<sub>x</sub>, Li/SVO, and Li/I<sub>2</sub> primary batteries for biomedical applications. While we mainly explore them as primary batteries, the literature on enhancing their reversibility as secondary batteries will also be reviewed for possible future applications in rechargeable energy storage.

## 2. Lithium carbon monofluoride

### 2.1. Working principles

The Li/CF<sub>x</sub> system, firstly reported by Matsushita Electric Industrial Company in Osaka, Japan, was one of the first commercially used solid-cathode battery, and ever since it was introduced, it has drawn significant attention for its outstanding energy density [5,6]. The overall discharge reaction in Li-CF<sub>x</sub> batteries can be expressed as.



$x = 1$  for stoichiometric carbon monofluoride compound. The theoretical specific capacities of the anode and the cathode are 3860 and 865 mAh/g, respectively, and the volumetric capacities are 2061 and 2335 mAh/cm<sup>3</sup> [3], respectively [7,8]. Given the theoretical voltage of 3.2 V, the overall theoretical specific energy and energy density are 2119 Wh/kg and 5830 Wh/L, respectively, which are almost the highest among all solid cathode system [2]. The current commercial Li/CF<sub>x</sub> battery could reach 260–780 Wh/kg based on the whole cell, depending on the physical design and size. Despite its outstanding energy density, Li/CF<sub>x</sub> battery has also offered a wide operating temperature range, safe operation, and long service/shelf life.

The CF<sub>x</sub> cathode is usually prepared by the fluorination of carbon sources, such as graphite. It has two basic phases, CF<sub>1</sub>, where fluorine atoms are inserted between two carbon layers with a CFCFC sequence and CF<sub>0.5</sub>, where fluorine atoms are inserted between every two pairs of carbon layers with a CCFCCFCC sequence, as shown in Fig. 2(a) [8]. CF<sub>x</sub> compound is described by a mix of both phases when  $x$  is between 0.5 and 1. Although CF<sub>x</sub> could yield a theoretical capacity of 865 mAh/g as a cathode, in a complete lithium battery system, the ultrahigh-capacity characteristic of Li/CF<sub>x</sub> is greatly limited by several factors. When  $x$  approaches 1, C–F covalent bond length decreases from 0.3 nm to 0.141 nm, and ionic/covalent nature of C–F bond makes it insulating and hard to yield expected discharge performance as a cathode. The inherently high electrical resistivity and slow diffusion of solvated lithium ions cause several shortcomings of the Li/CF<sub>x</sub> battery system, such as

low discharge rate, extra heat generation, and significant voltage drop at the initial discharging stage, especially at higher rates. Nowadays, the industry has pushed the current Li/CF<sub>x</sub> battery design to a theoretical limit through integrating a hybrid cathode and customized inner battery structure, and it keeps getting harder to use traditional methods to further improve its electrochemical performance. Luckily with the new insights gained in nanoscale material properties, it is possible to continue exploring possibilities in improving its discharging power capabilities and overall energy density.

Different from traditional fluorination methods, current nanotechnology researches mainly focus on improving electrical conductivity in CF<sub>x</sub> cathode by using nanostructured materials, such as nanosized carbon source for fluorination (e.g. carbon nanotubes and ball-milled graphite), advanced carbon additives, and nanoscale carbon coating. These methods can reduce the transport distance of electrons and improve electrical conductivity, leading to better power capability of the CF<sub>x</sub> electrode.

## 2.2. Nanocarbon host for fluorination

Jayasinghe et al. explored using MWCNT as the carbon source and avoided using highly toxic F<sub>2</sub> gas [9]. MWCNTs were fluorinated inside a customized plasma system with CF<sub>4</sub> gas under controlled conditions of 10 sccm flow rate, 5 torr pressure, and 150 °C temperature. Such a strategy has several advantages. First, MWCNTs' excellent electrical conductivity, as well as ideal surface area

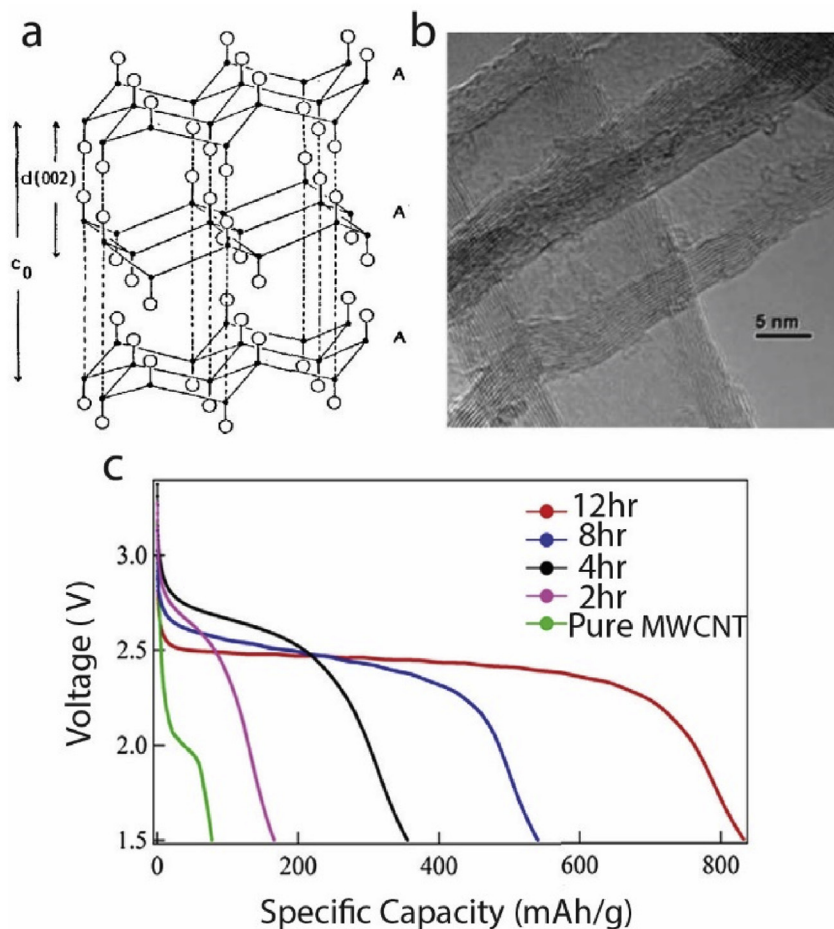


**Fig. 2.** (a) The crystal structure of carbon monofluoride [6]. (b) A TEM image of MWCNTs after fluorination [7]. (c) The discharge voltage profile of fluorinated MWCNT with various fluorination durations [7]. Adapted with permission from [6,7].

properties improved energy density and rate capabilities of Li/CF<sub>x</sub> battery, especially under high rate conditions. Second, the low-temperature fluorine intercalation technique created gaps on the CNTs that benefited the lithium-ion diffusion, and non-reacted carbons promoted electron flow efficiency with its excellent electrical conductivity. The electrochemical performance of such fluorinated MWCNTs are shown in Fig. 2(c). The specific capacity was considerably improved following the increase in fluorination duration. While pure MWCNT sample barely yielded a specific capacity around 100 mAh g<sup>-1</sup>, 12-h fluorinated MWCNT sample carried out the highest capacity exceeding 815 mAh g<sup>-1</sup>, reaching 95% of the theoretical capacity of 864 mAh g<sup>-1</sup>. The fluorinated MWCNT also showed a higher capacity at a high discharge rate compared to pure MWCNT. For the capacity at a high discharging current density of 1.5 A g<sup>-1</sup>, a 2-hr fluorinated sample yielded 172 mAh g<sup>-1</sup> capacity, which is at least 40% more than that of pure MWCNT sample. Meanwhile, the application of nanostructured MWCNT on battery electrodes also turns conventionally nonrechargeable Li/CF<sub>x</sub> battery to rechargeable, which probably arises from the ultra-small diameter of MWCNTs. For ~30 cycles, the charge/discharge experiments have demonstrated a 60.2% capacity retention for a 2-hr fluorinated sample and only 23% for pure MWCNT sample.

In addition to carbon nanotubes, Damien et al. found graphene an attractive carbon source for fluorination to improve energy density, power density, and faradic yield of Li/CF<sub>x</sub> battery [10]. Wittingham et al.'s research indicates that during Li/CF<sub>x</sub> battery discharging process, an intermediate phase named graphite intercalation compound (GIC) is involved, which includes solvated lithium ions and fluorinated graphite and obstructs the solvated lithium ions diffusion [11]. Now through using fluorinated graphene with very low fluorine content ( $x = 0.22$ ), different from graphite that has multiple atomic layers, it could phenomenally reduce the GIC layer thickness and improve the solvated lithium diffusion kinetics. Also, without the layered structure, fluorinated graphene helps concentrate more F atoms on the surface, which are more accessible to the lithium ions during the discharging process and further improve the energy density and faradic yield of Li/CF<sub>x</sub> system. The specific capacity of 767 mAh/g is observed for Li/CF<sub>x</sub>-FG (fluorinated graphene) sample while only 550 mAh/g for Li/(CF<sub>0.25</sub>)<sub>n</sub> sample at a current density of 10 mA/g. It is not hard to conclude that the FG-based battery has achieved over 40% more specific capacity of fluorinated graphite-based battery under all discharging current densities.

Fluorinated carbon nanofibers through static fluorination were realized by Ahmad et al. to increase synthesis yield and to prepare a larger amount of materials [12]. The higher amount of carbon that could be fluorinated by introducing pure fluorine gas through small and successive additions of fluorine gas at a lower temperature in a closed reactor leads to a decrease in the fluorination temperature. The as-prepared CF<sub>x</sub> battery reached capacity as 748 mAh g<sup>-1</sup> with 98% faradic yield. This static method protected the carbonaceous matrix from decomposition during fluorination, and then enhanced the energy density because of the increase of both the faradic yield and the discharge potential.

Ahmad et al. used fluorinated nanostructured carbon nanodiscs to push the theoretical limit of Li-CF<sub>x</sub> batteries [13]. When fluorinated ratio  $x$  approaches 1.0, the theoretical capacity of CF<sub>x</sub> will touch 865 mAh g<sup>-1</sup>. However,  $x$  higher than 1 may not mean higher capacity since excessive F will introduce more -CF<sub>2</sub> and -CF<sub>3</sub>, which are usually on sheet edges or structural defects and are inactive during the electrochemical process [14]. In order to limit CF<sub>2</sub> and CF<sub>3</sub> formation, the concept of "sub-fluorination" has been introduced. By using controlled fluorination through solid fluorinating agent TbF<sub>4</sub>, carbon nanodiscs showed decreased structural defects, and therefore, less -CF<sub>2</sub> and -CF<sub>3</sub>. The controlled-TbF<sub>4</sub>

fluorinated carbon nanodiscs showed F:C molar ratio as 0.95, and impressive capacity as 978 mAh g<sup>-1</sup> when coupled with Li anode.

### 2.3. Nanographite-based CF<sub>x</sub>

Besides utilizing nanoscale carbon host, a more direct and simpler way to improve Li/CF<sub>x</sub> battery performance is through breaking CF<sub>x</sub> particles to the nanoscale. M. Anji Reddy et al. conducted an experiment in using ball-milling techniques to specifically improve the Li-CF<sub>x</sub> battery discharging performance at a high discharge rate [15]. The pristine sizes of CF<sub>x</sub> particles are around 1–10 μm, and higher rotational speed (200–400 rpm) carries out a smaller particle size. The BET surface area increased from 213 m<sup>2</sup> g<sup>-1</sup> to 267 m<sup>2</sup> g<sup>-1</sup> during ball milling, and pore volume increased from 0.1 to up to 0.148 cm<sup>3</sup> g<sup>-1</sup> accompany with fewer micropores and more mesopores. Take 300 rpm as an example (Fig. 3(a)), the tap density increased from 0.3 g cm<sup>-3</sup> (pristine powder) to 1.07 g cm<sup>-3</sup>, which is ~40% of the theoretical density of CF<sub>x</sub> (2.82–2.88 g cm<sup>-3</sup>, for  $x = 1$ ) [15]. While the ball-milled sample showed slightly improved discharging capacity under the discharge rate of C/10, 1 C and 2 C, as shown in Fig. 3(a), it yielded an absolutely higher discharging capacity under a high discharge rate of 4 C and higher. At 4 C, the energy density of the milled sample (~600 mAh/g) almost doubled that of the pristine sample (~300 mAh/g). At 6 C, the 300-rpm sample delivered 40% of its nominal capacity, a power density of 9860 W/kg, and a gravimetric energy density of 800 Wh/kg, while the pristine sample could not yield any countable capacity in the studied voltage range. Surprisingly, the ball-milled sample still shows decent capacity under 6 C, while the pristine CF<sub>x</sub> sample failed to provide any effective discharging capacity.

The team also observes that smaller particles size do not always yield better electrochemical performance, as those ball-milled at 400 rpm show a lower energy density compared to that at 300 rpm under almost all discharge current rates, as shown in Fig. 3(b). This is attributed to that the crystal structure of CF<sub>x</sub> was destroyed at higher rotational speed, which results in a decrease in the internal electronic conductivity of carbon. Overall, through reducing the particle size by the ball milling process, the Li-CF<sub>x</sub> batteries could achieve a better discharging performance, especially at a higher discharge rate than before, and that result was accompanied by an even higher power capacity and specific energy density as well.

### 2.4. Nanostructure carbon as an additive, current collector and innovative structure base

In addition to nanostructuring active materials, carbon-based nanomaterials, such as CNTs, can also be used as conductive additives and conductive substrate in CF<sub>x</sub> cathode, as CNT has extremely high electrical conductivity (10<sup>6</sup>–10<sup>7</sup> S m<sup>-1</sup>)<sup>66</sup> and high thermal conductivity (>300 W m<sup>-1</sup> K<sup>-1</sup>)<sup>67–69</sup>. Qing Zhang et al. have added CNTs in Li/CF<sub>x</sub> system as conductive additives to enhance electrochemical performance [5]. One of the main challenges in their studies is that CNTs tend to aggregate together as bundles under natural state, due to the strong inter-tube interactions. For solving this problem, high-energy ball milling has been conducted to disperse CNTs and mix them with CF<sub>x</sub> samples. With 8% CNTs, after ball milling for 10 min, the cathode impedance drops dramatically from >300 Ω to less than 20 Ω. Ball milling breaks CF<sub>x</sub> particles and CNTs, and thus, yielding a larger contact area for CF<sub>x</sub> with CNTs. Longer milling time causes lower conductivity as the process might break the CNTs particle even smaller and shorter, which may cause particle aggregation. In contrast, when traditional super p carbon black is used, the cathode impedance only reduces to around 200 Ω, which is almost 10 times that of the CNTs/CF<sub>x</sub> sample. The lower

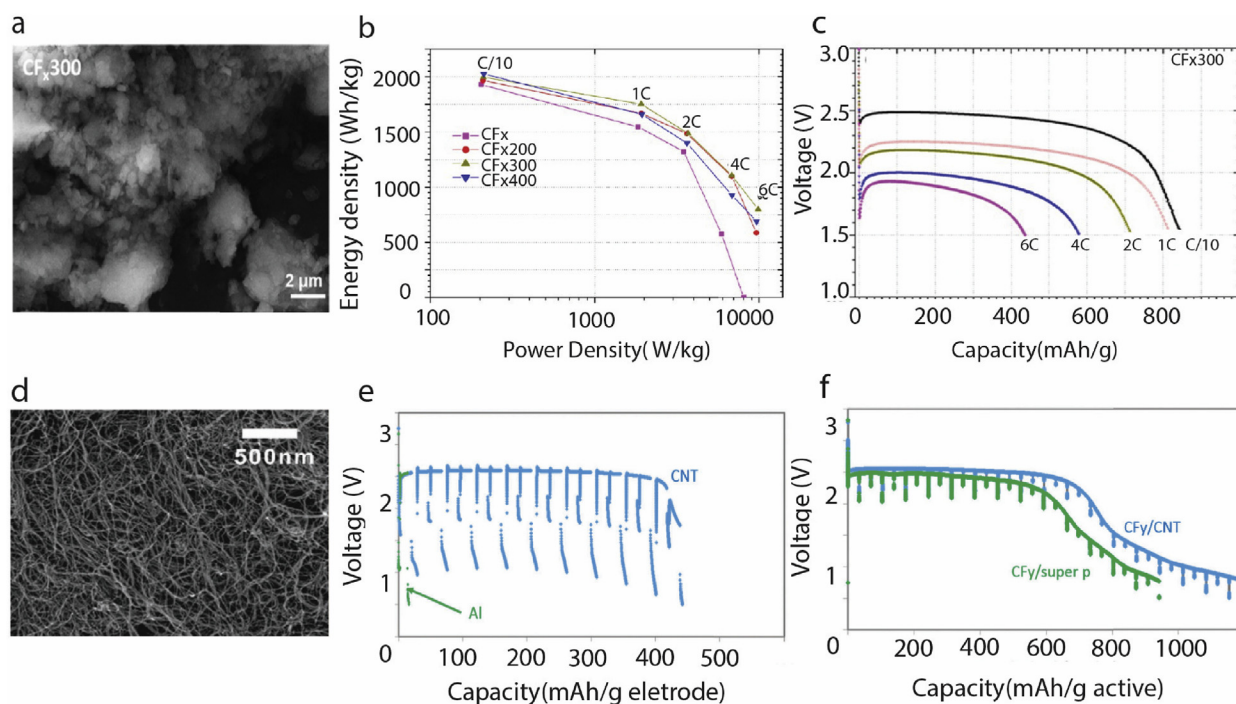


**Fig. 3.** (a) An SEM image of the CF<sub>x</sub> sample after 300 rpm ball milling [15]. (b) The energy and power densities comparison for CF<sub>x</sub> samples with ball milling rpm [5,15]. (c) The voltage profile of 300 rpm milled samples under different discharging rates [8,15]. (d) An SEM image of the CNT paper substrate [5]. (e) The voltage profile of Li/CF<sub>x</sub> batteries with CNT substrate and Al foil samples under the pulse discharging condition of 0.06/20/50 mA cm<sup>-2</sup> [5]. (f) The voltage profile for sandwich-like cathode structure with formula 1 and 2 correspondingly [5,11]. Adapted with permission from [5,11].

impedance also translates into better power capability. With the same mass loading of conductive additives, CF<sub>x</sub>/CNTs cathode could achieve a much higher conductivity, which means it also requires less mass loading to form a conductive network and potentially provide more space for cathode active material.

On the other side, CNTs can also be used as current collector instead of conventional Al substrate, which provides both longer operation time and higher voltage retention at pulse current, which are both critical for biomedical applications. As-prepared CNTs are shown in Fig. 3(d). First, under constant discharging condition, the capacity of CNTs sample doubled Al foil sample when discharging under 1 V. Moreover, just say at a pulse of 0.06/20/50 mA cm<sup>-2</sup>, the CNT sample could sustain the same background discharge voltage as the constant discharging condition of 0.06 mA cm<sup>-2</sup> condition, but Al foil sample could not provide any effective electrical power output after first high-current pulse, as shown in Fig. 3(e).

Based on the extraordinary performance of CNTs as a current collector and as conductive additives, a novel sandwich-like CF<sub>x</sub> cathode structure based on CNTs is proposed. As shown in the configuration below, the electrode structure is formed by attaching two CNTs substrates on both sides of the middle layer carbon monofluoride composite, which includes a mixture of CF<sub>x</sub> and CNTs additives. The experiment results in Fig. 3(f) have shown that a novel sandwich cathode structure could achieve a significant reduction of the initial voltage delay issue of traditional Li/CF<sub>x</sub> battery [5]. With further optimizing electrode density and other properties, CNTs are an attractive material for enhancing the performance of practical Li/CF<sub>x</sub> batteries.

## 2.5. Summary

These studies focusing on altering electrode material particle sizes and modifying electrode structures have been proven to be

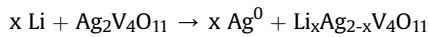
effective in improving Li/CF<sub>x</sub> specific energy and energy density, as well as eliminating voltage delay and heat generation problems. Based on the results, nanostructuring is a promising research direction and a possible approach to be applied in the industry to further extend battery longevity in implantable medical devices. Furthermore, when integrating these innovative approaches to the hybrid CF<sub>x</sub> battery cells such as Li-CF<sub>x</sub>/SVO or Li-CF<sub>x</sub>/MnO<sub>2</sub> [3,16]. It could achieve an even better discharging performance.

## 3. Silver vanadium oxide

### 3.1. Working principles

Similar to cardiac pacemakers that monitor heart rhythm and use electrical pulses to control the heartbeat rate within a safe range, implantable cardioverter defibrillators (ICDs) deliver electrical shocks when abnormal rhythms are detected to restore the normal heartbeat rate. Then, it is not hard to speculate that for ICDs, they demand primary batteries as their power sources to provide even higher power when triggered to deliver electrical shock as high as 10 W (2–3 A), which is equivalent to 1–2 C rate, and still not losing the high energy density for supporting the daily sensing mechanisms of devices with 5- to 9-year longevity [3]. Although Li/CF<sub>x</sub> stands out for its considerable high energy density, it fails to provide required power density to drive ICDs for high power electrical shocks. The lithium/silver vanadium oxide (SVO) system has drawn significant attention in meeting these requirements as the main power source to deliver remarkable discharging power with the benefit of the high electric conductivity nature of silver in the system. Besides, Li/SVO battery has a stepped voltage-capacity curve with a plateau near the end of discharge, making it a reliable end-of-service warning for device replacement prior to battery depletion.

Normally three forms of SVOs are discussed regarding the application as battery cathode:  $\text{AgVO}_3$ ,  $\text{Ag}_2\text{V}_4\text{O}_{11}$ , and  $\text{Ag}_4\text{V}_2\text{O}_7$  [17]. Among them,  $\text{Ag}_2\text{V}_4\text{O}_{11}$ , as shown in Fig. 4(a) for its crystal structure, is the one that has been used in industry for its lower self-discharging rate, as well as higher specific density ( $932 \text{ Wh kg}^{-1}$ ). The electrochemical reaction of Li-SVO batteries can thus, be found as:



While  $x$  denotes the moles of  $\text{Li}^+$  intercalated in the material, as  $x$  in the range of  $0 < x < 2.4$ , two silver cations of  $\text{Ag}_2\text{V}_4\text{O}_{11}$  are reduced from  $\text{Ag}(I)$  to  $\text{Ag}(0)$  at initial voltage of 3.25 V and formed metallic silver, which considerably improve the conductivity of the cathode and contribute to the high discharging power capability [18]. As  $x$  exceeds 2.4, the reduction of vanadium induced the formation of mixed-valent cathode material [17–19]. Bulk  $\text{Ag}_2\text{V}_4\text{O}_{11}$  can intercalate up to 7 mol of lithium per molecular unit ( $x = 7$ ), rendering a theoretical capacity of 315 mAh/g corresponding to  $x$  of 2.4.

One of the main challenges broadly applying SVO material toward other industrial fields is its limited energy density comparing to other high-density primary batteries, such as  $\text{Li}/\text{CF}_x$  and capacity loss at high loads and high depths of discharge. The main reason behind this is the severe diffusion transport limitation for the insertion of lithium, leading to a higher internal electrical resistivity and further compromise the discharge performance, such as energy densities and power capabilities. One direct solution to the diffusion limitation problem in the solid phase is to reduce the particle size to nanoscale, which increases the surface-to-volume ratio and

decreases the transport distance for charge motion. Researchers have studied this field regarding the application of several morphologies, such as nanowire, nanorods, nanocrystals, as well as a more sophisticated coaxial structure with conducting polymers. Meanwhile, for its ideal power and energy density, SVO has drawn more and more attention in rechargeable batteries [20]. However, because of the irreversible reduction of  $\text{Ag}^+$ , recognized in general, owing to ionic radii mismatch between  $\text{Ag}^+$  and  $\text{Li}^+$  ( $r_{\text{Ag}^+} = 1.15 \text{ \AA}$  vs.  $r_{\text{Li}^+} = 0.76 \text{ \AA}$ ), it has been discussed and reported to lose 80% of its capacity within 20 charge/discharge cycles [21,22]. Through introducing nanoscale material structure and morphology modification, SVO has exhibited unexpected reversible silver displacement reaction, achieving significant improvement in capacity and rate performance within certain cycles.

### 3.2. Electrochemical performance of nanoscale SVO system

In Jun Chen et al.'s research, a low-temperature hydrothermal method was introduced to synthesize SVO nanowires [23]. Instead of traditional solid-state thermal reaction synthesis method requiring 380–500 °C,  $\text{Ag}_2\text{V}_4\text{O}_{11}$  nanowires were prepared by hydrothermal method heating  $\text{V}_2\text{O}_5$ ,  $\text{Ag}_2\text{O}$  in the water at 180 °C for 24 h. In Fig. 4(b), the SEM image shows that  $\text{Ag}_2\text{V}_4\text{O}_{11}$  nanowire has a diameter of 30–50 nm. The electrochemical tests show that the pretreated nanowires provide a 3.52 V open-circuit voltage and 366 mAh/g specific discharge capacity down at 1.5 V at 37 °C, which are better than 3.32 V and 319 mAh/g of the bulk SVO sample [23]. Results confirmed that reducing SVO particle sizes leads to shorter diffusion path, faster reaction kinetics, and larger specific surface

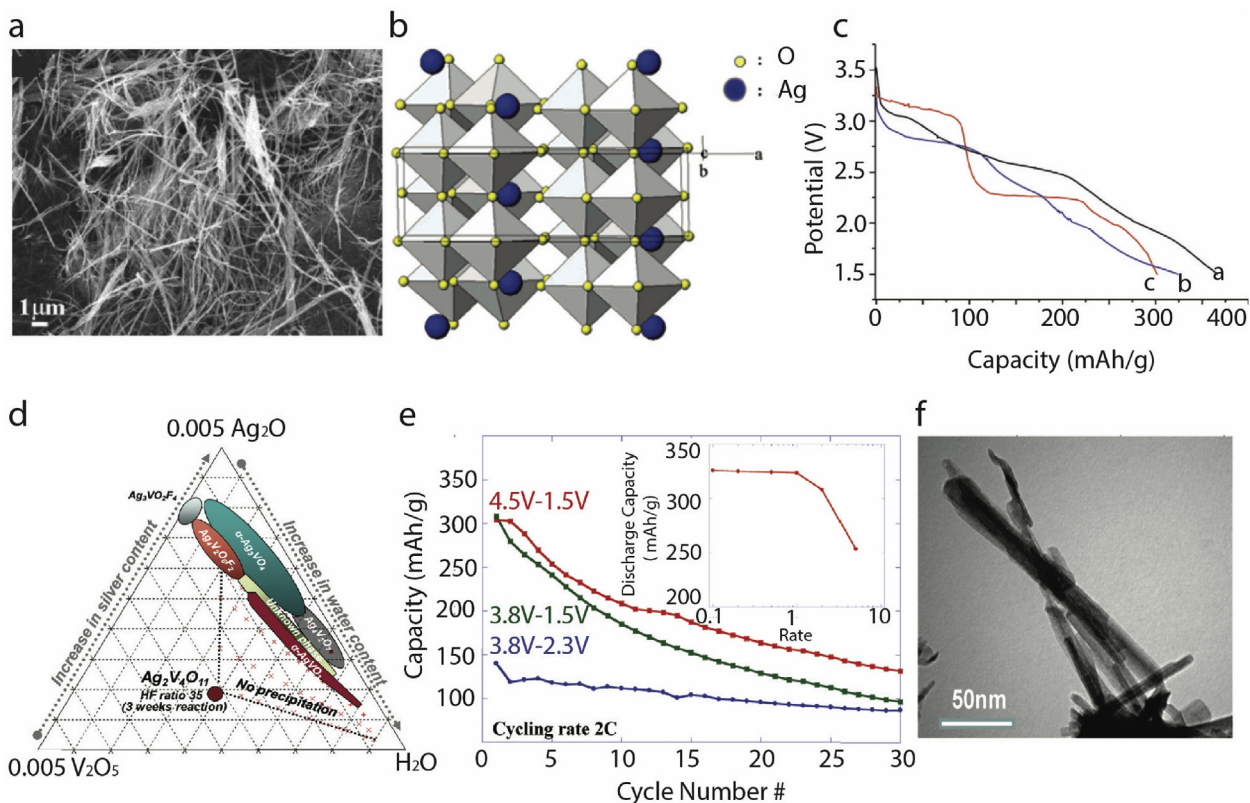


**Fig. 4.** (a) The Crystal structure of  $\text{Ag}_2\text{V}_4\text{O}_{11}$  [23]. (b) An SEM image of as-pretreated  $\text{Ag}_2\text{V}_4\text{O}_{11}$  nanowires [23]. (c) The discharge curve as a function of the capacity of the  $\text{Ag}_2\text{V}_4\text{O}_{11}$  nanowire electrode (black line a) [23]. (d) Schema of the ternary diagram  $\text{Ag}_2\text{O}/\text{V}_2\text{O}_5/\text{HF}_{(\text{aq})}$  using a 30 equivalent ratio of HF as mineralizer [24]. (e) Capacity retention recorded on composite SVO electrode at 2C conditions for different cycling potential windows. The influence of the cycling rate on the electrode capacity from 0.1 to 5 C is shown in the inset [24]. (f) TEM demonstrates acicular particle morphology with a size of 10–15 nm wide and 50–200 nm long [23,24]. Adapted with permission from [19,20].

area to contact with active materials, and thus, results in an overall improvement in battery capacity and discharge potential.

Previous experimental results by Jun Chen et al. were collected under a low current discharging condition (0.01 mA), but for cardiac pacing and ICDs, instantaneous current shocks up to 1C are also needed without losing the ~4.3 Ah capacity of current commercial Li/SVO batteries. Besides, even though the synthetic temperature has been reduced greatly, it still faces a considerable challenge toward application in industry. To further lower the required temperature for synthesizing SVO nanostructure, as well as investigating its performance under a high discharge rate, Poepelmeier et al.'s group introduced a ternary system to synthesize SVO nanocrystal at room temperature [24]. The precursors of SVO are  $\text{Ag}_2\text{O}$ ,  $\text{V}_2\text{O}_5$ , and  $\text{HF}_{(\text{aq})}$ , which play significant roles in the stoichiometry of final products. The as-synthesized SVO nanorods have an acicular morphology with  $10\text{--}15 \times 50\text{--}200$  nm in size, as shown in Fig. 4(f). The SVO nanocrystal cathode yields a cathode capacity of 320–325 mAh/g below 1C, 305 mAh/g at 2C, and 252 mAh/g at 5C, which are quite considering theoretical cathode capacity 315 mAh/g. Besides,  $\text{Ag}_2\text{V}_4\text{O}_{11}$  nanorods exhibit much better capacity retention over cycles with reversible silver displacement reaction and  $\text{V}^{5+}/\text{V}^{3+}$  redox activity. At a high rate of 2 C, although capacity still drops a little due to lack of reversibility in the  $\text{V}^{5+}/\text{V}^{3+}$  redox couple, SVO nanocrystals could maintain a much better capacity over 30 charge/discharge cycles especially in the range of 3.8 V and 2.3 V like shown in Fig. 4(e). There is still considerable room to be improved, such as the efficiency of  $\text{V}^{5+}/\text{V}^{3+}$  redox couple and electrochemical dissolution of the reoxidized silver ions in the electrolyte, which will further improve in capacity retention for Li/SVO battery.

### 3.3. Reversibility studies of crystal structure on lithium-ion intercalation

Although there is still a long way to go applying SVO toward rechargeable battery, several innovative morphologies, and in-depth structure studies have enlightened the potential and possibilities. Wu et al. investigated the relationship between the vanadium oxide matrix and the reversibility of reduced silver in the Li/SVO system [20]. The hydrothermal method, combined with the electrospinning technique, provides  $\beta\text{-Ag}_{0.33}\text{V}_2\text{O}_5$  nanorods (NRs) with the flower-like nanostructure. Through constructing atomic inter-planar linkages that are less likely to collapse after extraction/insertion of silver ions, a more stable crystal structure was realized in  $\beta\text{-SVO}$  NRS. Test results show an improved cycling stability with a capacity loss of only  $1 \text{ mA h g}^{-1}$  per cycle after 30 runs at a current of  $20 \text{ mA g}^{-1}$ , which is considerable comparing to bulk sample that been reported lost 80% of its capacity within 20 cycles [25].

### 3.4. SVO/conductive polymer hybrid system

Based on results achieved regarding morphologies modification in nanoscale SVO, innovative nanostructures were proposed to integrate with these structures, and hence, further improve its electrochemical performance in a battery. Yunlong Zhao et al. proposed a novel coaxial nanostructure for  $\beta\text{-AgVO}_3$  with PANI (polyaniline) conductive polymers aiming to provide better cathode conductivity and prevent transition metal dissolution in an electrolyte. A  $\beta\text{-AgVO}_3$  core surrounding by PANI outer layers formed the coaxial nanowire structure. Samples are prepared by successively adding liquid aniline monomers to as-prepared  $\beta\text{-AgVO}_3$  nanowire-immersed water solution. Later, the same molar weight to ammonium of persulfate is added for reaction and dried to obtain SVO/PANI triaxial nanowires. As shown in Fig. 5(a), the diameter of the triaxial nanowire is around 80 nm, with a thickness

of PANI coating around 8 nm, and the wire is decorated with silver nanoparticles with a diameter of ~30 nm. The electrochemical performances of such structure with different amount of polyaniline were tested between 1.5 and 4 V versus  $\text{Li}^+/\text{Li}$ . As shown in Fig. 5(b), while all SVO/PANI samples demonstrate better discharge capacity than pristine  $\text{AgVO}_3$  sample, 50 wt% sample show the highest initial capacity and after 20 cycles, which are 211 and 131 mAh/g, both higher than those of pristine  $\beta\text{-AgVO}_3$  nanowires without polyaniline, which are 199 and 76 mAh/g (with 20th cycle capacity retention of 41.7%). The reason for that might attribute to the thick and uneven PANI layer generated when too much aniline monomer added in the synthesis process. With an appropriate adjustment in the weight percentage of aniline, the coaxial SVO/PANI nanowire structure has been proved to be a valid and effective tool to improve the SVO electrochemical performance as a battery cathode material.

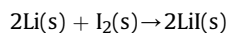
### 3.5. Summary

For alleviating diffusion transport limitation in the solid phase, the SVO particle sizes are reduced to nanoscale to provide a larger surface area, higher lithium ions diffusion rates, and faster electronic kinetics. To moderate irreversible silver ion reduction from amorphous vanadium oxide matrix, a flower-like nanorods structure was designed with inter-planar constructions, which created void channels for  $\text{Ag}^+$  to transfer through the interstices and diffuse with a higher degree of freedom [20]. From basic nanostructure to the composite coaxial nanowire, the insight gained through altering SVO morphologies has provided a new direction to explore more possibilities in further improving Li/SVO system and applying SVO toward more industry with its excellent power and energy density.

## 4. Lithium iodine

### 4.1. Principle of Li/I<sub>2</sub> battery

The year 2019, marks the forty-seventh anniversary of the first human cardiac pacemaker implant powered by a lithium battery; a lithium-iodine (Li/I<sub>2</sub>) cell [27]. Before its invention in 1972, cardiac pacemakers were powered by nickel-cadmium and zinc-mercury batteries, which only had less than two-year longevity [28]. Its appearance soon dominated the biomedical industry for its excellent longevity of 10 years, no gas generation, adaptable shape and sizes, corrosion resistance, minimum weight, excellent current drain [29]. Standard cell reaction of Li/I<sub>2</sub> battery is given below:



The overall reaction yields an open-circuit potential of 2.8 V [2]. Although the main compositions of cathode iodine and polyvinylpyridine (PVP) are not electricity conductive by themselves, they form a conductive charge-transfer complex when mixed and heated together [29]. The ratio of iodine to PVP is typically between 30:1 and 50:1 depends on manufacturers. When such complex contacts the lithium metal anode, it immediately forms a monomolecular layer of crystalline lithium iodine (LiI), which acts as both separator and solid electrolyte.

On the other side, one significant drawback for the system is the low ionic conductivity of the solid LiI layer that jeopardizes the overall power density, as well as capacity. More importantly, along with cell discharging, the LiI layer increases its thickness and thus further increases internal impedance. Fig. 6(a) shows the voltage versus capacity results collected from ADD (accelerated discharge data) testing, which use series of constant resistive loads to predict

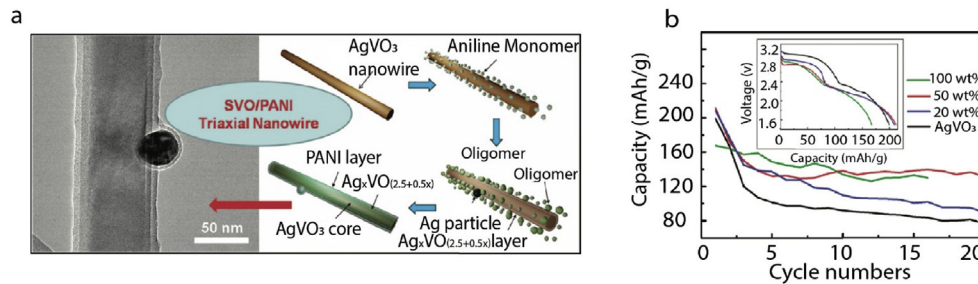


**Fig. 5.** (a) Schematic illustration of the formation of SVO/PANI triaxial nanowire. (b) Capacity vs. cycle number curves and first discharge curves (inset) of  $\beta$ - $\text{AgVO}_3$  and SVO/PANI nanowire with different amount of polyaniline [26]. Adapted with permission from [22].

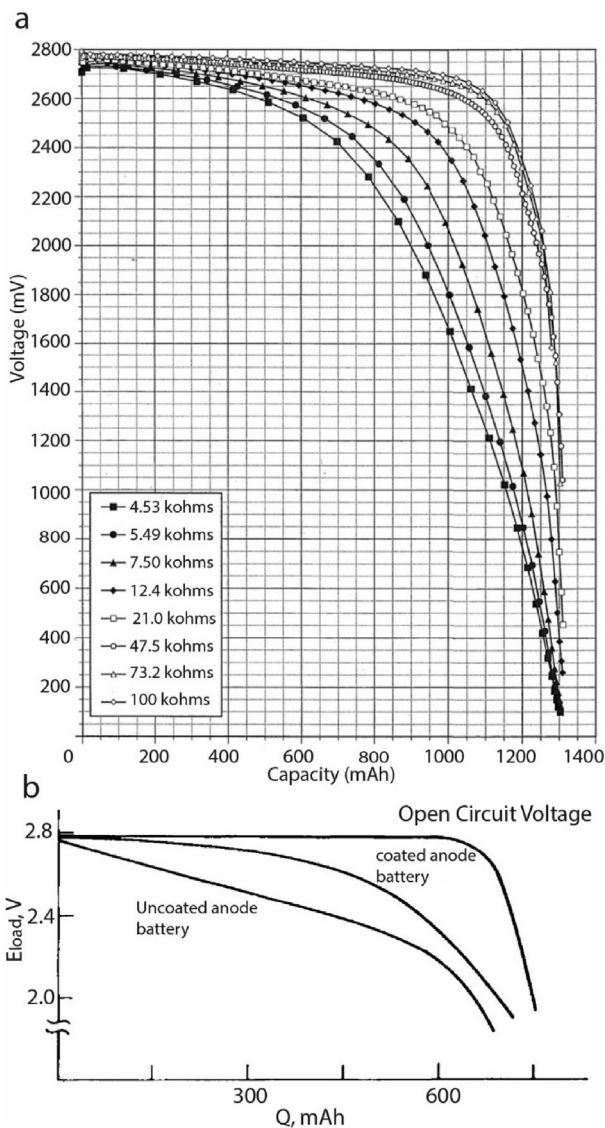


**Fig. 6.** (a) Constant Resistive Load discharge of groups of lithium/iodine-PVP batteries discharged at loads ranging from 4.52 kOhms to 100 kOhms [26]. (b) Load voltage versus discharge state for uncoated and P2VP-coated anode  $\text{Li}/\text{I}_2$  batteries discharged at  $6.7 \mu\text{A}/\text{cm}^2$   $37^\circ\text{C}$ .<sup>2,30</sup> Adapted with permission from [2,26].

the performance of batteries under extremely low current conditions present in cardiac pacemaker application. It is quite obvious to observe the gradual and predictable voltage decrease pattern induced by increasing in  $\text{LiI}$  impedance that allows scientists and

clinical personnel to monitor the real-time depth of discharge and predict expected battery life in order to schedule replacement surgery for maximum safety [30].

Several improvements have been achieved in the industry in improving battery performance by lowering the internal  $\text{LiI}$  electrolyte impedance. For alleviating such negative impacts on battery performance, one solution was proposed in 1976 by Mead et al. by adding a poly-2-vinylpyridine (P2VP) coating on the lithium metal anode [31]. The anode coating, first prepared by the brush-coating technique, was examined under scanning electron microscopy and rendered macro and microstructural differences between the structures of the  $\text{LiI}$  formed in the cell reaction, leading to an obvious decrease in internal impedance and increase in discharging voltage, as shown in Fig. 6(b) [2]. While  $\text{Li}/\text{I}_2$  system is generally regarded as solid-state systems, P2VP coating triggers a liquid reaction among  $\text{LiI}$ ,  $\text{I}_2$ , and P2VP and induces a liquid phase that improves the ionic conductivity of  $\text{LiI}$  of one to two orders of magnitude higher [1]. The brush-coating technique was later replaced by a substrate-coating method, which yields an even better coating uniformity, lower self-discharging rate, and better current-delivery capability [30].

Today, the power requirements for implantable medical devices and other implantable medical devices has increased considerably from microwatts range to milliwatts along with more functions and sensing mechanism, and thus,  $\text{Li}/\text{CF}_x$  and  $\text{Li}/\text{SVO}$  systems that discussed above are preferred regarding their higher power and energy densities than  $\text{Li}/\text{I}_2$  system. For its superior reliability and safety, today,  $\text{Li}/\text{I}_2$  remains the choice of power source for many implantable medical devices [30]. But to adapt to the high power consumption of current medical devices, it must be improved to produce a higher power density, as well as better cycling performance if it is adapted into rechargeable batteries. Current research on  $\text{Li}-\text{I}_2$  is more focused on rechargeable system and nanostructured electrodes that enhance the power density. In this review, we focus on the development of nanostructured electrodes for improving the power capability of the  $\text{Li}-\text{I}_2$  system, which has great potential to be used on implantable batteries.

#### 4.2. $\text{Li}/\text{I}_2$ battery with aqueous electrolyte

Hye Ryung Byon et al.'s team proposed a 3D nanoarchitected current collector design for aqueous iodine cathode, where the redox is between  $\text{I}^{3-}$  and  $\text{I}^-$  [32]. The nanoarchitected current collector can shorten the diffusion length of redox couples, and thus, improve the electrochemical performance. A vertically aligned multi-walled carbon nanotube (VACNT) is the basis of such structure since it has lightweight, high electronic conductivity, and fast kinetics due to catalytic effects induced by the oxygen functional groups inside. The VACNT, prepared by chemical vapor deposition on the quartz substrate, has multiple carbon nanotube

walls with diameters of 30–100 nm aligned vertically to form an overall structure with a thickness of 1 mm and pore size of 2.73 nm. The SEM image of the VACNT structure is shown in Fig. 7(a) below. The VACNT mat current collector on Ti is filled with aqueous cathode and KI to use as the cathode for a Li-I<sub>2</sub> hybrid redox battery, which has Li metal with 1 M of LiPF<sub>6</sub> in ethylene carbonate (EC)/dimethyl carbonate (DMC) electrolyte for the anode and a ceramic separator LATP to separate liquid electrolyte for the cathode and the anode.

As shown in Fig. 7(b), the first cycle yielded 206 mAh/g initial capacity at 2.5 mA cm<sup>-2</sup>, which keeps a 103% of theoretical capacity of Li/I<sub>2</sub> battery and reasonably drops to 185 mAh/g for the following cycles (2–200 cycles) because of the stranded Li<sup>+</sup> ions and idle I<sub>3</sub><sup>-</sup>. Such a system then shows surprisingly stable cycling performance with excellent capacity retention rate cycles (185 ± 3 mAh/g), steady charge/discharge potentials, and high Coulombic efficiency (100 ± 0.5%) for 200 cycles [33]. The battery yielded an energy density of 330 W h/kg and 650 W h/L. Such improvement and performance in cycling stability and energy density are attributed to the use of carbon nanotube-based current collector and make it attractive as rechargeable batteries for biomedical devices, but manufacturing challenges in separating organic and aqueous electrolyte must be addressed first.

In the example above, the employment of nanostructured current collectors indeed achieved significant improvement in rate capability, as well as cycling performance, but how to separate the organic electrolyte and the aqueous electrolyte is a challenge for scaling up. On the other side, a solid iodine electrode has also been studied. Zhao et al. conducted an experiment building an I<sub>2</sub> cathode by adsorbing iodine ions into 1 nm pores in nanoporous carbon cloth [34]. In this design, nanoporous carbon cloth is chosen to be combined with iodine that helps improve the overall electrochemical performance of the cathode. Such cathode is prepared through a “solution-absorption” process that enables nanoporous carbon cloth with average 1 nm pores absorbing iodine ions in aqueous solution. Then the iodine/nanoporous carbon electrode is combined with lithium metal anode in an ether-based electrolyte

with LiNO<sub>3</sub>. The as-prepared cathode shows excellent high-rate performance, as shown in Fig. 7(c) with capacities of 301, 273, 232, 169 mAh/g at 0.5, 1, 2 and 5 C discharging rate respectively [34]. With the benefit of nanoporous structure of nanoporous carbon cloth providing extra intercalation space for lithium ions, the as-prepared cathode was tested and exhibited an initial discharge capacity of 299 mAh/g, which reaches 142% of the theoretical capacity of traditional iodine cathode. The energy density reaches 475 Wh/kg, which is a lot higher than 330 Wh/kg of the triiodide/iodide redox cathode system [33,35]. In spite of a lower retention rate of 65% (195 mAh/g after 300 cycles), the overall discharge performance results clearly out beat the aqueous triiodide/iodide cathode in the way of better capacity and energy density.

#### 4.3. Summary

Lithium iodine battery has been described as an “elegant” battery system for its simple reaction of lithium and iodine, yet involves complex internal structure in the cathode, such as iodine and PVP to form an electronic conductor, as well as triiodide/iodide redox couple like discussed above [30]. While utilizing the high energy density generated by lithium iodine reaction, approaches have been conducted to improve the overall performance regarding different aspects. While aqueous triiodide/iodide cathode could significantly improve the cycling performance and rate capability toward an ideal rechargeable system, carbon cloth-based Li/I<sub>2</sub> is preferred as it can use a single electrolyte, reducing complication in architecting the electrolyte. It is not hard to conclude that both nano approaches have their own way of improving the Li/I<sub>2</sub> battery adapting higher power requirements of implantable medical devices. More methods based on those structures could be further investigated, such as applying the aqueous triiodide/iodide couple to nanoporous carbon cloth, using a more effective electrolyte or a more chemically stable separator and they would certainly benefit the Li/I<sub>2</sub> system and helps it adapt the power requirements of current commercial implantable medical devices.

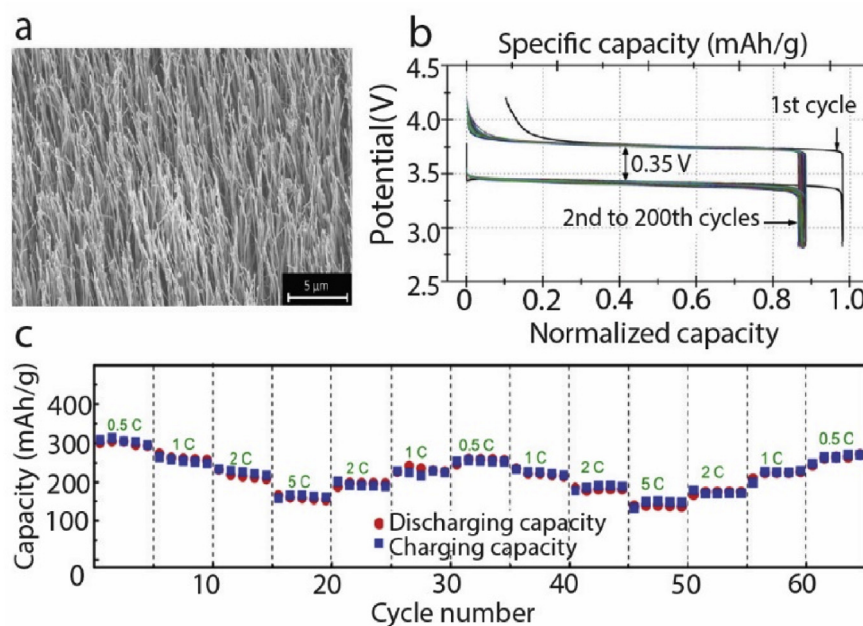


**Fig. 7.** (a) An SEM image of VACNTs [29]. (b) Charge/discharge profiles at a current rate of 2.5 mA cm<sup>-2</sup> at 298 K [29]. (c) Rate performance with equal mass solid-state iodine cathode on nonporous carbon cloth [33,34]. Adapted with permission from [29,30].

**Table 2**  
Nanomethods in improving primary battery performance.

	Nanostructure	Morphology	Pristine cathode performance	Nanostructured performance	Conditions
Li/CF <sub>x</sub>	carbon source	MWCNT	N/A	815 mAh/g	N/A
		graphene	550 mAh/g	767 mAh/g	10 mA/g
	cathode	N/A	300 mAh/g	600 mAh/g	4C
	additive	CNTs	>300 Ω	20 Ω	N/A
	current collector	CNTs	292 mAh/g	392 mAh/g	0.2/4/8 mA/cm <sup>2</sup>
Li/SVO	structure base	sandwich-structure	N/A	Improved initial voltage delay	N/A
	cathode	nanowire	319 mAh/g	366 mAh/g	0.01 mA
		nanorod	315 mAh/g (theoretical)	305 mAh/g	2C
Li/I <sub>2</sub>	coaxial structure	PANI	199 mAh/g	211 mAh/g	20 cycles
	current collector	VACNTs	211 mAh/g (theoretical)	206 mAh/g	2.5 mA/cm <sup>2</sup>
	cathode	nonporous cloth	211 mAh/g (theoretical)	299 mAh/g	0.5C

## 5. Conclusion and perspective

For medical devices, especially for implantable ones, batteries play a significantly important role in providing seamless power to support the continuous sensing and treating operation of devices. Since the first development of lithium/iodine system, it has been extensively used for its simple cell structure and high energy density at low rate, but as the capacity and energy density requirements rise with more advanced implantable medical devices, its limited capacity at higher rate became the biggest drawback and gained less attention in recent years. Meanwhile, Li/CF<sub>x</sub> system improved the energy density by almost three times compared to that of the lithium/iodine system and yielded significant enhancement in working performance under pulse discharging conditions, which particularly favors the application for powering a cardiac pacemaker. However, the initial voltage delay, abrupt voltage declines near the end of battery life, and limited power density toward other high-power consumption medical devices, such as the cardiac defibrillator remain unsolved. The Li/SVO system, on the other hand, solves these issues at the cost of lower energy density comparing to Li/CF<sub>x</sub> and Li/I<sub>2</sub>. With the goal of finding a balance among safety, energy and power density as the ultimate solution for implantable medical devices, hybrid systems, such as the Li/CF<sub>x</sub>-SVO hybrid-cathode battery, were developed with comparable energy density to Li/I<sub>2</sub>, but with about two orders of magnitude greater power density [36]. Currently Li-CF<sub>x</sub>, Li-SVO, and their hybrids are widely used for craniological disease applications.

Using nanostructured materials, such as carbon nanotubes and nanowires, not only addresses internal material challenges, such as high charge transfer impedance in CF<sub>x</sub> and slow ion diffusion in SVO but also alleviates the irreversibility of ion transfer between these primary battery electrodes and enables potential application toward a rechargeable system to extend longevity even longer. A summary table of the improvement made on the battery system is shown in Table 2 below.

Meanwhile, since the tapping density of nanomaterials is usually lower than conventional micron-sized materials, which will sacrifice the volumetric energy density of the battery, the application of nanomaterials in implantable devices should be carefully considered. One possible solution is to use a mixture of micron-sized and nanomaterials together, where nanoparticles fill voids among micron-sized particles. Hence, the sacrifice of energy density is hereby limited. It is worth mentioning that some novel systems, such as Mg and Zn based batteries, have made significant progress in recent years [37,38]. Although Mg and Zn are indeed safer than Li to human body, the low capacities of cathodes in Zn or Mg batteries (mostly below 200 mAh g<sup>-1</sup>), together with low voltage, seriously hinder their applications in small implantable medical devices. Thus, it is reasonable to conclude that primary

lithium batteries will still dominate this field of study for a very long period of time with their high energy densities and capacities.

In current Li-CF<sub>x</sub>, Li-SVO, and Li-MnO<sub>2</sub> batteries for implantable applications, the flammable organic liquid electrolyte is still used, which could cause severe issues if there is a leakage or thermal runaway [39]. It would be ideal for replacing flammable liquid electrolytes with solid-state electrolytes, which are much safer. For solid electrolytes, potential candidates include PEO [40], LATP [41], garnet type Li<sub>7</sub>La<sub>3</sub>Zr<sub>2</sub>O<sub>12</sub> (LLZO) [42], and sulfide electrolytes [43]. However, the poor contact of the interfaces between SSEs and electrodes limits their applications [44], having negative impacts, such as the high interfacial resistance between the cathode and Li metal. Thus, further improvements are needed to incorporate solid electrolyte into implantable batteries.

Meanwhile, the development of more advanced implantable medical devices, such as dual-chamber leadless cardiac pacemakers, is still limited by the size and longevity of their power sources. After all, there is a theoretical limit for primary lithium battery, and a lot of recent research were conducted regarding transforming kinetic energy like blood flow, muscle movement as potential energy source to charge the battery inside human bodies. Dagdeviren et al. tested a piezoelectric energy harvester on the outer surface of the heart, and Wang et al. designed a triboelectric nanogenerator based on the muscle movement of breathing, and both designs achieved enough energy to power a cardiac pacemaker [45,46]. Thus, it is promising to continue exploring the possibility of lithium battery in not just the field of energy density, but also their overall rechargeability performance.

In the future, more studies will be conducted investigating detailed reaction mechanisms in these materials and working effects of nanostructures on the crystal structure, reaction kinetics, and reversibility, which will lead to better battery designs with longer operational time, higher power capability, and safer working environment for biomedical devices.

## Declaration of competing interest

The authors have no conflict of interest.

## Acknowledgements

The authors have no conflict of interest and acknowledge support from Columbia University.

## References

- [1] D.C. Bock, A.C. Marschilok, K.J. Takeuchi, E.S. Takeuchi, Batteries used to power implantable biomedical devices, *Electrochim. Acta* 84 (2012) 155–164.
- [2] T.B. Reddy, *Linden's Handbook of Batteries*, vol. 4, McGraw-hill, New York, 2011.

- [3] P. Gomadam, et al., Modeling Li/CF<sub>x</sub>-SVO Hybrid-Cathode Batteries, vol. 154, 2007.
- [4] J. Marple, Performance characteristics of Li/MnO<sub>2</sub>-CF<sub>x</sub> hybrid cathode jellyroll cells, *J. Power Sources* 19 (1987) 325–335.
- [5] Q. Zhang, K.J. Takeuchi, E.S. Takeuchi, A.C. Marschilok, Progress towards high-power Li/CF<sub>x</sub> batteries: electrode architectures using carbon nanotubes with CF<sub>x</sub>, *Phys. Chem. Phys.* 17 (2015) 22504–22518.
- [6] C. Peng, et al., Ultrahigh-energy-density fluorinated calcinated macadamia nut shell cathode for lithium/fluorinated carbon batteries, *Carbon* 153 (2019) 783–791.
- [7] D. Lin, Y. Liu, Y. Cui, Reviving the lithium metal anode for high-energy batteries, *Nat. Nanotechnol.* 12 (2017) 194.
- [8] T. Nakajima, R. Hagiwara, K. Moriya, N. Watanabe, Discharge characteristics of poly (carbon monofluoride) prepared from the residual carbon obtained by thermal decomposition of poly (dicarbon monofluoride) and graphite oxide, *J. Electrochem. Soc.* 133 (1986) 1761–1766.
- [9] R. Jayasinghe, et al., Optimization of Multi-Walled Carbon Nanotube based CF<sub>x</sub> electrodes for improved primary and secondary battery performances, *J. Power Sources* 253 (2014) 404–411.
- [10] D. Damien, et al., Fluorinated graphene based electrodes for high performance primary lithium batteries, *RSC Adv.* 3 (2013) 25702–25706.
- [11] M.S. Whittingham, Mechanism of reduction of the fluorographite cathode, *J. Electrochem. Soc.* 122 (1975) 526–527.
- [12] Y. Ahmad, K. Guérin, M. Dubois, W. Zhang, A. Hamwi, Enhanced performances in primary lithium batteries of fluorinated carbon nanofibers through static fluorination, *Electrochim. Acta* 114 (2013) 142–151.
- [13] Y. Ahmad, M. Dubois, K. Guérin, A. Hamwi, W. Zhang, Pushing the theoretical limit of Li-CF<sub>x</sub> batteries using fluorinated nanostructured carbon nanodiscs, *Carbon* 94 (2015) 1061–1070.
- [14] S. Chen, et al., Ideal gas thermodynamic properties of six fluoroethanes, *J. Phys. Chem. Ref. Data* 4 (1975) 441–456.
- [15] M.A. Reddy, B. Breitung, M. Fichtner, Improving the energy density and power density of CF<sub>x</sub> by mechanical milling: a primary lithium battery electrode, *ACS Appl. Mater. Interfaces* 5 (2013) 11207–11211.
- [16] Zhang, X. & Wang, X. High Capacity and High Rate Lithium Cells with CF<sub>x</sub>-MnO<sub>2</sub> Hybrid Cathode. U.S. patent (2009).
- [17] F. Cheng, J. Chen, Transition metal vanadium oxides and vanadate materials for lithium batteries, *J. Mater. Chem.* 21 (2011) 9841–9848.
- [18] R. Ramasamy, C. Feger, T. Strange, B. Popov, Discharge characteristics of silver vanadium oxide cathodes, *J. Appl. Electrochem.* 36 (2006) 487–497.
- [19] E.S. Takeuchi, W.C. Thiebolt, The reduction of silver vanadium oxide in lithium/silver vanadium oxide cells, *J. Electrochem. Soc.* 135 (1988) 2691–2694.
- [20] Y. Wu, et al., Highly improved rechargeable stability for lithium/silver vanadium oxide battery induced via electrospinning technique, *J. Mater. Chem.* 1 (2013) 852–859.
- [21] K.J. Takeuchi, A.C. Marschilok, S.M. Davis, R.A. Leising, E.S. Takeuchi, Silver vanadium oxides and related battery applications, *Coord. Chem. Rev.* 219 (2001) 283–310.
- [22] R.D. Shannon, Revised effective ionic radii and systematic studies of interatomic distances in halides and chalcogenides, *Acta Crystallogr. - Sect. A Cryst. Phys. Diffr. Theor. Gen. Crystallogr.* 32 (1976) 751–767.
- [23] S. Zhang, W. Li, C. Li, J. Chen, Synthesis, characterization, and electrochemical properties of Ag<sub>2</sub>V<sub>4</sub>O<sub>11</sub> and AgVO<sub>3</sub> 1-D nano/microstructures, *J. Phys. Chem. B* 110 (2006) 24855–24863.
- [24] F. Sauvage, V. Bodenez, J.-M. Tarascon, K.R. Poeppelmeier, Room-temperature synthesis leading to nanocrystalline Ag<sub>2</sub>V<sub>4</sub>O<sub>11</sub>, *J. Am. Chem. Soc.* 132 (2010) 6778–6782.
- [25] K. West, A. Crespi, Lithium insertion into silver vanadium oxide, Ag<sub>2</sub>V<sub>4</sub>O<sub>11</sub>, *J. Power Sources* 54 (1995) 334–337.
- [26] L. Mai, et al., Rational synthesis of silver vanadium oxides/polyaniline triaxial nanowires with enhanced electrochemical property, *Nano Lett.* 11 (2011) 4992–4996.
- [27] W. GREATBATCH, C.F. HOLMES, The lithium/iodine battery: a historical perspective, *Pacing Clin. Electrophysiol.* 15 (1992) 2034–2036.
- [28] G. Nelson, A brief history of cardiac pacing, *Tex. Heart Inst. J.* 20 (1993) 12.
- [29] V.S. Mallela, V. Ilankumar, N.S. Rao, Trends in cardiac pacemaker batteries, *Indian Pacing Electrophysiol. J.* 4 (2004) 201.
- [30] C. Holmes, The lithium/iodine-polyvinylpyridine pacemaker battery-35 years of successful clinical use, *ECS Trans.* 6 (2007) 1–7.
- [31] R.T. Mead, W. Greatbatch, F.W. Rudolph, Lithium-iodine Battery Having Coated Anode, U.S. patent, 1976.
- [32] Y. Zhao, L. Wang, H.R. Byon, High-performance rechargeable lithium-iodine batteries using triiodide/iodide redox couples in an aqueous cathode, *Nat. Commun.* 4 (2013) 1896.
- [33] Y. Zhao, et al., A 3.5 V lithium-iodine hybrid redox battery with vertically aligned carbon nanotube current collector, *Nano Lett.* 14 (2014) 1085–1092.
- [34] Q. Zhao, Y. Lu, Z. Zhu, Z. Tao, J. Chen, Rechargeable lithium-iodine batteries with iodine/nanoporous carbon cathode, *Nano Lett.* 15 (2015) 5982–5987.
- [35] B.B. Owens, P.M. Skarstad, D.F. Untereker, Solid electrolyte batteries. *Advances in electrochemistry and electrochemical engineering*, vol. 8, 1971, pp. 1–62.
- [36] D.F. Untereker, G. Jain, P.A. Tamirisa, J. Hossick-Schott, M. Viste, in *Clinical Cardiac Pacing, Defibrillation And Resynchronization Therapy*, Elsevier, 2017, pp. 251–269.
- [37] M. Mao, T. Gao, S. Hou, C. Wang, A critical review of cathodes for rechargeable Mg batteries, *Chem. Soc. Rev.* 47 (2018) 8804–8841.
- [38] F. Wang, et al., Highly reversible zinc metal anode for aqueous batteries, *Nat. Mater.* 17 (2018) 543.
- [39] T. Jin, et al., Nonflammable, low-cost, and fluorine-free solvent for liquid electrolyte of rechargeable lithium metal batteries, *ACS Appl. Mater. Interfaces* 11 (2019) 17333–17340.
- [40] Z. Xue, H. Dan, X. Xie, Poly(ethylene oxide)-based electrolytes for lithium-ion batteries, *J. Mater. Chem.* 3 (2015) 19218–19253.
- [41] Q. Cheng, et al., Stabilizing solid electrolyte-anode interface in Li-metal batteries by boron nitride-based nanocomposite coating, *Joule* 3 (2019) 1510–1522.
- [42] R. Murugan, V. Thangadurai, W. Weppner, Fast lithium ion conduction in garnet-type Li<sub>7</sub>La<sub>3</sub>Zr<sub>2</sub>O<sub>12</sub>, *Angew. Chem. Int. Ed.* 46 (2007) 7778–7781.
- [43] N. Kamaya, et al., A lithium superionic conductor, *Nat. Mater.* 10 (2011) 682–686.
- [44] J. Sakamoto, More pressure needed, *Nature Energy* 4 (2019) 827–828.
- [45] Q. Zheng, et al., In Vivo powering of pacemaker by breathing-driven implanted triboelectric nanogenerator, *Adv. Mater.* 26 (2014) 5851–5856.
- [46] C. Dagdeviren, et al., Conformal piezoelectric energy harvesting and storage from motions of the heart, lung, and diaphragm, *Proc. Natl. Acad. Sci.* 111 (2014) 1927–1932.